Near-Threshold Production of ω Mesons in the $pp \to pp\omega$ Reaction

F. Hibou,[1] O. Bing,[1] M. Boivin,[2] P. Courtat,[3] R. Gacougnolle,[3] Y. Le Bornec,[3] J. M. Martin,[3] F. Plouin,[2,4]
B. Tatischeff,[3] C. Wilkin,[5] N. Willis,[3] and R. Wurzinger[2,3]

[1]*Institut de Recherches Subatomiques, IN2P3-CNRS/Université Louis Pasteur, B.P. 28, F-67037 Strasbourg Cedex 2, France*
[2]*Laboratoire National Saturne, F-91191 Gif-sur-Yvette Cedex, France*
[3]*Institut de Physique Nucléaire, IN2P3-CNRS/Université Paris-Sud, F-91406 Orsay Cedex, France*
[4]*LPNHE, Ecole Polytechnique, F-91128 Palaiseau, France*
[5]*University College London, London WC1E 6BT, United Kingdom*

(Received 26 February 1999)

The total cross section for ω production in the $pp \to pp\omega$ reaction has been measured at 5 c.m. excess energies from 3.8 to 30 MeV. The energy dependence is easily understood in terms of a strong proton-proton final state interaction combined with a smearing over the width of the state. The ratio of near-threshold ϕ and ω production is, to within relatively large uncertainties, consistent with the predictions of a simple one-pion-exchange model. The degree of violation of the Okubo-Zweig-Iizuka rule is similar to that found in the $\pi^- p \to n\omega/\phi$ reactions.

For ideal mixing, where the ϕ meson is composed purely of strange quarks and the ω contains only up and down ones, the production of the ϕ by nonstrange hadrons is strongly suppressed by the Okubo-Zweig-Iizuka (OZI) rule [1], which forbids diagrams with disconnected quark lines. Deviations from ideal mixing are small and these suggest that, under similar kinematic conditions, the ratio R of single ϕ to ω production should be about $R \approx 4 \times 10^{-3}$ [2]. Values larger than this could be signals for hidden strangeness in some of the incident particles or due to intrinsic violations of the rule through second-order processes. The most striking enhancements have been seen in $\bar{p}p$ annihilation where, in certain channels, observed ϕ production rates [3] are up to 2 orders of magnitude higher than predicted by the rule.

Most reported violations are much more modest. Typical of these is the recent comparison of ω and ϕ production in proton-proton collisions by the DISTO collaboration at 2.85 GeV [4]. The ratio of the measured production cross sections is $\sigma_T(pp \to pp\phi)/\sigma_T(pp \to pp\omega) = (3.7 \pm 1.3) \times 10^{-3}$ which, after correcting for phase space effects, leads to an OZI enhancement of about an order of magnitude. Because of the large ϕ/ω mass difference, such corrections are model dependent since the excess energy Q (the kinetic energy in the final state) is 320 MeV for the ω, but only 82 MeV for the ϕ. While s and p final waves might suffice for the ϕ, many partial waves are likely to contribute to ω production. Any OZI test really requires a dynamical model, but the simplest empirical approach might be to compare rates at the same value of Q, where the angular momentum barriers are similar, rather than at the same beam energy. We here report measurements of the ω production cross section in the range $3.8 \le Q \le 30$ MeV. Though somewhat below the DISTO Q-value, these data suggest that the OZI enhancement is little different to that seen in $\pi^- p \to n\omega/\phi$ [5].

The data were taken at the Laboratoire National Saturne as part of a program of measuring near-threshold meson production in $pp \to ppX$ by detecting two protons in SPESIII, a large acceptance magnetic spectrometer, and identifying the meson X as a missing mass peak. Experimental conditions were similar to those pertaining to the production of the η and η' [6], and so only essential features are reported.

The ω production has been measured at nominal incident proton energies T_p of 1905, 1920, 1935, 1950, and 1980 MeV using a liquid hydrogen target of 270 mg/cm^2 thickness. The beam intensity was measured and controlled during the runs through an ionization chamber placed in the beam downstream of the target and two scintillator telescopes viewing the target. These monitors were calibrated using the standard carbon activation technique [7]. In order to estimate the background under the expected ω peak, data were also taken at 1865 MeV, where ω production should be negligible.

Under standard SPESIII conditions, the momentum range of the analyzed particles is $600 \le p \le 1400$ MeV/c, the momentum resolution $(0.5-1.0) \times 10^{-3}$, and the effective solid angle acceptance per particle $\Delta\Omega \approx 10^{-2}$ sr. The associated detection system, which provides good resolution over the full acceptance of the spectrometer together with multiparticle detection possibilities, includes three multiwire drift chambers and four planes of scintillators as the trigger. The first of these chambers is located near the focal surface, inclined with respect to the optical axis of the spectrometer. Since the ω width is 8.4 MeV/c^2, particle tracks could be reconstructed, to well within the required momentum and missing mass resolution, using information purely from this chamber.

For near-threshold meson production, it is important to verify the values of T_p or Q by independent means [6,8,9]. In one approach, we used the $pp \to d\pi^+$ and

$pp \rightarrow p\pi^+ n$ reactions to carry out simultaneously very accurate calibrations of the mean field of the spectrometer and measurements of the incident proton energy at each nominal energy. The neutron mass in the three-body final state is almost equally sensitive to T_p and the mean field, whereas the peak position of the deuteron is much more sensitive to the field. The experimental data were compared to the results of extensive numerical simulations, taking into account all of the details of the experimental setup and data-reduction algorithms. Incident proton energies measured by this method were slightly lower than nominal ones calculated using the parameters of the Saturne machine, with a mean difference of $\Delta T = T_{\text{nominal}} - T_{\text{measured}} = 1.1 \pm 0.8$ MeV. This offset is consistent with previous measurements [6,8,9] and we adopt it as a standard energy shift.

Typical missing mass spectra of the $pp \rightarrow ppX$ reaction are shown in Fig. 1. That in Fig. 1a, recorded at an incident energy $T = 1865$ MeV, shows a rather uniform multipion production shape, except for the enhancement near the kinematic limit. This arises from the combined effects of the increase in acceptance and the proton-proton final state interaction (FSI). Particle production in the target windows contributes typically 10% of the spectrum. These data have been used to extrapolate the background underneath the ω peak to the higher incident energies using the following procedure. Let β and β_n be c.m. velocities

at energies T and T_n respectively. The measured momenta and angles of the protons are first transformed, event-by-event, from the laboratory to the c.m. system with the velocity $-\beta$ and then transformed back to the laboratory with the velocity $+\beta_n$. Data recorded at $T_p = 2400$ MeV, just below the threshold for the $pp \rightarrow pp\eta'$ reaction [6], could be used to assess the reliability of the method; the results of this test are shown in Fig. 1b. The measured and predicted spectra are normalized to the same number of incident protons. Since the multipion production cross section will have changed somewhat over such a large incident energy difference, the agreement in magnitude and especially shape is noteworthy.

Experimental spectra (points with error bars) obtained at $T_p = 1920$ and 1980 MeV are presented in Figs. 1c and 1d, together with extrapolated background spectra (solid line histograms) and simulated ω peaks (smooth curves). To evaluate the number of $pp \rightarrow pp\omega$ events, the extrapolated background and ω peak were combined to fit the data in the ω peak region, and the results are represented by the dashed line histogram. It should, however, be noted that, at the higher energies, the background extrapolation method does not reproduce completely the observed end peak. The higher solid line histogram in Fig. 1d is obtained by subtracting the simulated ω peak from the experimental spectrum. The difference between the two solid line histograms thus represents the unexpected
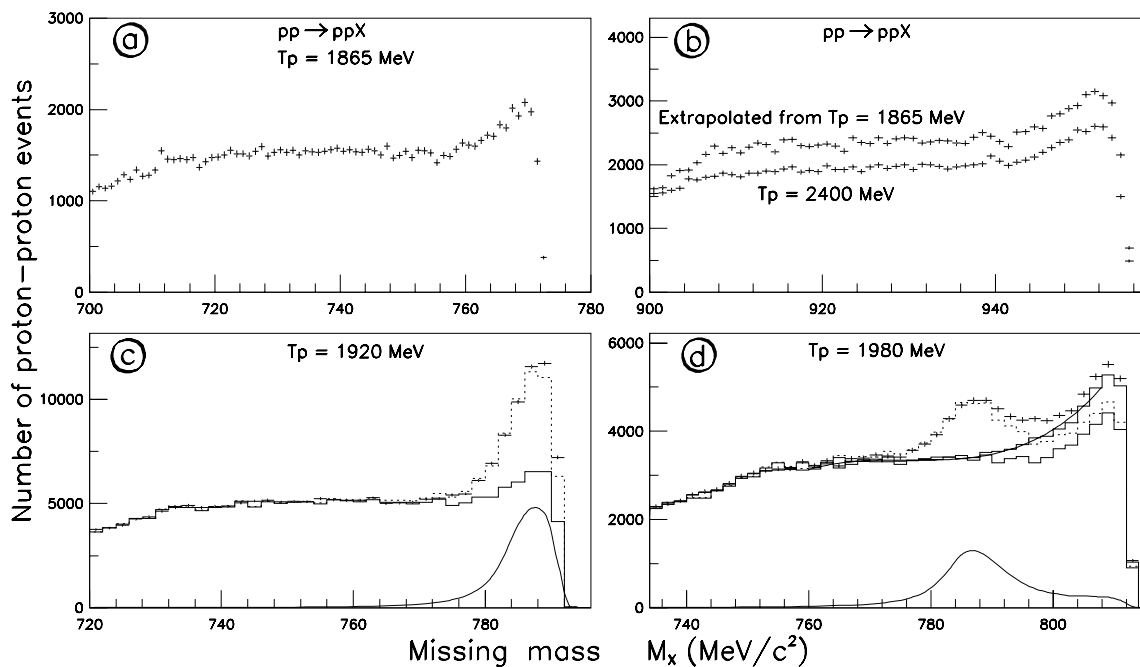

FIG. 1. Missing mass spectra of the $pp \rightarrow ppX$ reaction at nominal beam energies of (a) 1865 MeV, (b) 2400 MeV, (c) 1920 MeV, and (d) 1980 MeV. The spectrum in (a) has been used to generate the background at the higher energies. In (b) the spectrum measured at 2400 MeV is compared to the background extrapolated from 1865 MeV and normalized to the integrated beam intensity. In (c) and (d) the $pp \rightarrow ppX$ spectra are shown together with simulated ω distributions (smooth curves) and the extrapolated backgrounds (solid line histograms) which are combined (dashed line histograms) to fit the measured spectra. The higher solid line histogram in (d) is obtained by subtracting the simulated ω peak from the experimental spectrum. The smooth curve is a fit of this new background spectrum with a polynomial of degree 3.

enhancement of the background. At 1980 MeV, which was the highest incident energy, the mass of the ω was used as a free parameter to generate new background spectra. These were fit by polynomials and an example, of degree 3, is illustrated by the smooth curve in Fig. 1d. Such fits lead to a midtarget value of $Q = \sqrt{2m_p(T_p + 2m_p)} - (2m_p + m_\omega) = 29.1 \pm 1.4$ MeV, where m_p and m_ω are the masses of the proton and ω respectively, and T_p is also a mid-target figure. Using this value of Q, which is fixed by the production data themselves, together with $T_p = 1978.4$ MeV determined by the pion production results, a mass of $m_\omega = 784.0 \pm 1.4$ MeV is obtained. Imposing instead the compilation mass $m_\omega = 781.94 \pm 0.12$ MeV [10] gives a value of the excess energy $Q = 31.1 \pm 0.4$ MeV. This error bar might be underestimated since, due to dynamical effects, the apparent ω mass in hadronic production can easily change by some small fraction of the width [11]. The two Q determinations are broadly consistent and their mean is quoted in Table I at the highest T_p. Since small changes in T_p could be controlled to about 0.1 MeV, the values of Q closer to threshold were determined in terms of differences from this highest point.

Very near threshold, the angular and momentum acceptances of SPESIII cover the whole phase space for meson production in a single setting at $\theta_{lab} \approx 0°$, but angular cuts become important for $Q > 10$ MeV. In the $pp \rightarrow pp\omega$ reaction at $T_p = 1978.4$ MeV, for example, only 25% of detected events have an ω angle lying within $45° < \theta_{cm} < 135°$. At the energies of our experiment, the angular variations induced by higher partial waves in the final state are expected to be small. Even at $Q = 82$ MeV the angular distribution of ϕ production is fairly flat [4]. The value of the total cross section can then be determined provided that the final state interaction between the two emerging protons in the $1S_0$ state is taken carefully into account when determining the acceptance [6]. The dominance of this FSI in the differential distributions is seen in η production at $Q = 37$ MeV [12].

Another effect which must be included when estimating the acceptance for ω production at low energy is the finite width of the resonance. The excess energy Q is defined

with respect to the central ω mass value and, at the lowest Q, more than 30% of the Breit-Wigner distribution lies below the production threshold. On the other hand, even at $Q = 0$, the lower half of the meson can still be produced.

These two effects, the proton-proton FSI and the Breit-Wigner mass distribution, were introduced into the SPESIII Monte Carlo simulation used in calculating the acceptance. The total cross sections deduced at each mean value of Q are shown in Table I and Fig. 2. The errors arise mainly from uncertainties in the number of events in the ω peak (15%–27%), the number of incident protons, the target thickness, the detection efficiency and the dead time (in total 12.5%), and the acceptance (3.5%–7%), which includes that induced by the error on Q.

The large momentum transfer required for heavy meson production means that the amplitude is primarily sensitive to the short-range behavior in the pp system. In this limit, the energy dependence of the total cross section for the production of a stable ω meson is dominated by a three-body phase space modified by the pp FSI, and this leads to

$$\sigma_T(pp \rightarrow pp\omega) = C_\omega \left(\frac{Q/\epsilon}{1 + \sqrt{1 + Q/\epsilon}} \right)^2, \quad (1)$$

where, including Coulomb distortion, $\epsilon \approx 0.45$ MeV [13]. Details of the production dynamics are contained in C_ω, which is expected to be slowly varying.

Comparing this with our data in Fig. 2, it is seen that the predicted Q dependence is much too sharp. However, after smearing over an ω Breit-Wigner shape, this yields a
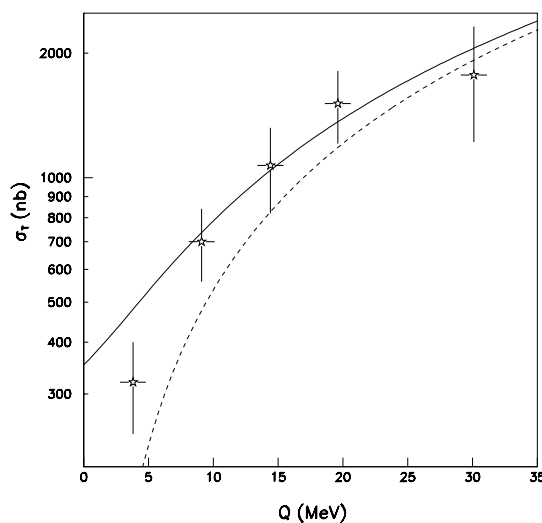

FIG. 2. Total cross section for $pp \rightarrow pp\omega$ as a function of the excess energy Q with respect to the nominal ω mass. The error bars comprise all of the statistical and known systematic uncertainties, including that induced by the error on Q. The broken curve is the prediction of Eq. (1) for a stable ω with $C_\omega = 37$ nb. The solid curve smears this result over a Breit-Wigner distribution with $\Gamma_\omega = 8.4$ MeV/c^2.

TABLE I. Total cross sections for the $pp \rightarrow pp\omega$ reaction measured near threshold. The excess energy Q with respect to the ω central mass value, having taken into account average energy losses of the beam in the target, has an uncertainty of ± 0.9 MeV. The cross section errors quoted are, respectively, statistical, that induced by the error on Q and the remaining known systematic uncertainties.

Q (MeV)	σ_T (μb)
3.8	$0.32 \pm 0.06 \pm 0.01 \pm 0.05$
9.1	$0.70 \pm 0.10 \pm 0.04 \pm 0.09$
14.4	$1.07 \pm 0.20 \pm 0.08 \pm 0.13$
19.6	$1.51 \pm 0.23 \pm 0.08 \pm 0.18$
30.1	$1.77 \pm 0.48 \pm 0.10 \pm 0.23$

much smoother energy dependence which reproduces well our results with the value of $C_\omega = (37 \pm 8)$ nb.

Direct comparison with the DISTO ϕ production data [4] is complicated because this group has not yet deduced absolute cross sections but only a ϕ/ω production ratio. Normalizing to old ω bubble chamber data taken at slightly higher energies [14], one finds that $\sigma_T(pp \to pp\phi) = (0.28 \pm 0.14)$ μb at $Q = 82$ MeV. Although there are uncertainties in extrapolating Eq. (1) to such high Q, the DISTO measurement would correspond to $C_\phi = (1.8 \pm 0.9)$ nb. Hence

$$R_{pp} = \frac{C_\phi}{C_\omega} = (4.9 \pm 2.6) \times 10^{-2}, \qquad (2)$$

to be compared with the OZI prediction of 4×10^{-3}. Most of the error in the enhancement factor of 12 ± 7 comes from the uncertainty in the DISTO normalization [4].

The ratio of ϕ to ω production has been measured near threshold in $\pi^- p$ collisions [5] and, at the same value of Q, gives

$$R_{\pi^- p} = \frac{\sigma_T(\pi^- p \to \phi n)}{\sigma_T(\pi^- p \to \omega n)} = (3.7 \pm 0.8) \times 10^{-2}. \quad (3)$$

An apparent ω threshold suppression, which might be kinematic in origin [15], has been corrected for.

A simple one-pion-exchange model describes *qualitatively* ratios of meson production in proton-proton collisions near threshold [6,16]. In this approach the ϕ/ω ratio can be obtained in terms of that measured in $\pi^- p$,

$$R_{pp} \approx \left(\frac{(2m_p + m_\omega)(m_p + m_\phi)}{(2m_p + m_\phi)(m_p + m_\omega)} \right)^{3/2} \left(\frac{m_\omega}{m_\phi} \right) R_{\pi^- p}$$

$$\approx 0.82 \times R_{\pi^- p} = (3.0 \pm 0.7) \times 10^{-2}, \qquad (4)$$

where m_ϕ is the ϕ mass.

The striking agreement between Eqs. (2) and (4) must be considered to be rather fortuitous in view of the large experimental *and* theoretical uncertainties. Nevertheless, both the $\pi^- p$ and pp experiments do suggest strongly that the OZI enhancement is about an order of magnitude,

in line with the original DISTO analysis at the same beam energy [4]. Further experimental work is clearly needed in order to establish good absolute normalizations, but it would also help if the ω and ϕ data points were measured closer in Q. However, understanding the theoretical significance in the proton-proton case requires a more sophisticated model than naive one-pion exchange [17].

[1] G. Zweig, CERN Report 8419/Th, 1964, p. 412; S. Okubo, Phys. Lett. **5**, 165 (1965); I. Iizuka, Prog. Theor. Phys. Suppl. **37–38**, 21 (1966).
[2] H. J. Lipkin, Phys. Lett. **60B**, 371 (1976); J. Ellis, M. Karliner, D. E. Kharzeev, and M. G. Sapozhnikov, Phys. Lett. B **353**, 319 (1995).
[3] C. Amsler *et al.,* Phys. Lett. B **346**, 363 (1995).
[4] F. Balestra *et al.,* Phys. Rev. Lett. **81**, 4572 (1998).
[5] D. M. Binnie *et al.,* Phys. Rev. D **8**, 2789 (1973); J. Keyne *et al.,* Phys. Rev. D **14**, 28 (1976).
[6] A. M. Bergdolt *et al.,* Phys. Rev. D **48**, R2969 (1993); A. Taleb, Ph.D. thesis, Université Louis Pasteur, Strasbourg, 1994 (CRN 94-61); F. Hibou *et al.,* Phys. Lett. B **438**, 41 (1998).
[7] J. Banaigs *et al.,* Nucl. Instrum. Methods **95**, 1479 (1971).
[8] F. Plouin *et al.,* Phys. Lett. B **276**, 526 (1992).
[9] N. Willis *et al.,* Phys. Lett. B **406**, 14 (1997).
[10] C. Caso *et al.,* Eur. Phys. J. C **3**, 633 (1998).
[11] R. Wurzinger *et al.,* Phys. Rev. C **51**, R443 (1995).
[12] H. Calén *et al.,* TSL/ISV-98-0198 (to be published).
[13] G. Fäldt and C. Wilkin, Phys. Lett. B **382**, 209 (1996).
[14] L. Bodini *et al.,* Nuovo Cimento A **58**, 475 (1968).
[15] C. Hanhart and A. Kudryavtsev, nucl-th/9812022 (to be published).
[16] C. Wilkin, in *Proceedings of the 8th International Conference on the Structure of Baryons, Bonn, 1998,* edited by D. W. Menze (World Scientific, Singapore, 1999), p. 505 (nucl-th/9810047).
[17] K. Nakayama *et al.,* Phys. Rev. C **57**, 1580 (1998).